PPPL--2644

DE89 017747

Image Simulation Using LOCUS

J.D. Strachan and J.A. Roberts
Princeton Plasma Physics Laboratory
Princeton, New Jersey 08543

The LOCUS data base program has been used to simulate images and to solve simple equations. This has been accomplished by making each record (which normally would represent a data entry) represent sequenced or random number pairs.

Introduction

One of the most widely used computer programs at PPPL is the LOCUS (Refs.1,2) data base program. It is even used by several other fusion labs. Some reasons for its popularity include its usefulness as a depository for data, flexibility in processing data, ease of use, the ability to form mathematical relations with the data, and the large number of graphical and statistical options available that make the handling and analysis of data easy and comprehensive. These features are useful in other computations besides data base work, which motivated our use of the LOCUS data base for different computations.

In this paper, we document our attempts at making LOCUS perform (1) image simulations and (2) computational solutions of ordinary equations. LOCUS is not presently optimized nor even efficient (in terms of computer processing) for these applications. However, for the physicist, the LOCUS program quickly yields results in a format that is particularly useful since it includes the LOCUS graphical and statistical packages.

The image simulations were used to reveal some features of the TFTR pictures of detached plasmas. A model that consisted of a thin radiating shell which had uniform emissivity on its surface was found that reproduced those pictures. The equation solutions were used to indicate reasons for the stability and formation of detached plasmas. We found that the evolution from a MARFE to a detailed plasma might be explained by the radiation curve with the postulate that T_e at the plasma edge was decreasing.

Data Base Setup

The data base (PICT1) was set up with each record consisting of three numbers: PH1 TH, and RA. PH1 is a number from 0.0 to 1.4 in steps of 0.02. For each value of PH1, there is a separate record for TH from 0 to 6.2 in steps of 0.1 so that a matrix of 70 × 62 = 4340 records is created. This means that a mesh of data points is available in the PICT1 (Fig.1). Associated with each record is the number RA, which is a two-digit random number. The result is that two different sets of random numbers can be generated by considering RA and PH1 to be independent variables (Fig.2) or by considering RA and TH to be independent variables (Fig.3). In the examples reported here, we used the random number (RA) to randomize one or both of the sequenced numbers.

Thus, the character of PICT1 is different from typical LOCUS data bases in that there is no actual data in PICT1. PICT1 consists only of sets of numbers which allow one range of numbers (sequenced or randomized) to be plotted against another range of numbers. We have found applications for a LOCUS data base having such a matrix of numbers.

Image of Detached Plasma

We used the PICT1 data base to simulate the plasma TV pictures (Ref. 4) of the detached plasma (Fig.4). The plasma TV camera views through a TFTR window pointed at the moveable limiter blades at Bay M (Fig. 4a). For comparison, a small diameter compression plasma image (Fig. 4b) demonstrates the effect of the limiter (either inside wall or moveable limiter) contact. This image is exposed for times covering the pre- and post-compressed plasma.

The picture of the detached plasma (Fig. 4d) has several features which initially puzzled us. In particular, the bright region on the inside edge indicated possible inner wall recycling. It also seemed somehow consistent with the bolometer signals which had indicated uniform surface emission from the detached plasma (Ref. 5). Similarly, the fuzzy region at the top and bottom indicated possible recycling from the blades of the moveable limiter.

Our image modelling using PICT1 reproduced all the significant features of the detached plasma (Fig. 4d). The data points were distributed uniformly on a toroidal surface and projected from the perspective of the plasma TV camera (Fig. 4c).

This image was formed from the coordinates

$$\begin{aligned} Y &= A \frac{\sin(TH)}{\{[A \sin(TH)]^2 + [x_1 + \cos(PH1)(R + A \cos(TH))]^2 + [Z1 + (\sin(PH2)[R + A \cos(TH)])]^2\}^{1/2}} \qquad (1) \\ X &= arctan \left(\frac{x_1 + (\cos(PH2)[R + A \cos(TH)])}{Z_1 + (\sin(PH1)[R + A \cos(TH)])} \right), \end{aligned}$$

where x_1 and Z_1 are the positions where the picture is viewed, and R and A are the major and minor radius of the toroid.

The generated image can have the points easily randomized on the surface by the simple transformation of TH going to $TH + 2 \times 10^{-3} RA$ and $PH1$ going to $PH1 + 10^{-3} RA$ (Figs. 5 and 6). Such a view avoids the duplication of points in the image near the turning points. Similarly, other images can be easily formed (e.g., a cylinder in Fig. 7). On the actual study of the detached plasmas, images were formed with poloidal and toroidal localization at the limiters (either moveable or inner wall). As well, the thickness of the radiating shell was varied and even a volume emission was simulated (Fig. 8) by placing the points uniformly throughout the plasma volume.

All of these examples were easily accomplished due basically to the utility and user friendly nature of the LOCUS database program.

Solution of Simple Equations

We have found that the PICT1 type of LOCUS data base also provides quick graphical and statistical access to solutions of simple equations. Again in studying the detached plasmas, we wanted to find plausible mechanisms for the evolution of the boundary from the MARFE to the symmetrically radiating detached state (Ref. 6). The conservation equations on the outside magnetic surface are (as written by Drake in Ref. 7)

$$\begin{aligned}
\frac{\partial n}{\partial t} &+ \mathbf{b}\cdot\nabla n v_{\parallel} = 0 \\
m_i n \frac{\partial v_{\parallel}}{\partial t} &= -\mathbf{b}\nabla \mathbf{p} \\
\frac{3}{2} n \frac{\partial T}{\partial t} &- \mathbf{b}\cdot\nabla k_{\parallel} \mathbf{b}\cdot\nabla T - \nabla_{\perp}\cdot k_{\perp} \nabla_{\perp} T \\
&= -nT\,\mathbf{b}\cdot\nabla v_{\parallel} + H - L.
\end{aligned}$$

To explore the plausible formation mechanisms of the detached plasma, we reduced these equations (by several approximations) to

$$\begin{aligned}
\frac{\partial P_{\parallel}}{q^2} T_T^{3/2} (T_M + T_T^2)^2 &- P_{OH}(T_T + T_M)^2 - \frac{3a}{2\nabla \tau_E} N T_M (T_M + T_T) \\
&- R N^2 T_T^2 \exp\left\{ -\frac{(T_M - \xi)^2}{2\phi} \right\} = 0, \qquad (2)
\end{aligned}$$

where $P_{||}$, Q, P_{OH}, a, ∇, τ_E, N, R, ξ, and ϕ are known constants. T_T is the electron temperature on the outside magnetic surface in the non-Marfe region, and T_M is the electron temperature in the Marfe. The ratio of the two temperatures is an indication of the Marfe and the detached plasma.

Even though the above equation has been simplified by several physical assumptions, analytic solution is difficult. We solve the equation using the PICT1 data base by letting T_T be described by one of the variables. In the graphs shown, we used

$$TT = \frac{0.7 - (PH1)/2}{0.006}$$

in order to simulate the range of possible electron temperatures. A time scale could be applied to the simulation on the basis of typical current decay rates used to form TFTR detached plasmas. In this case,

$$TIME = 0.2(PH1).$$

Now at each time (or equivalently, at each value of TT), we want to solve the equation for TM. This was done by making an expression for Eq. (2) (say F) and by letting the other variable represent the possible values of TM. In this case, we used

$$TM = TT - 10(TH) + 0.01(RA).$$

Thus, solutions to the equation are obtained at any one time (equivalently, any one value of PH1) by those values for TM (equivalently, TH) that are close to F = 0 (Fig. 9). The evolution of the solution describes only a few of the available matrix of PH1, TH number pairs (Fig. 1). These solutions are identified simply in LOCUS by making the solution to the equation be those points where the equation is close to zero. For example, the units of Eq. (2) are in MW since it is a power balance equation and in Fig. 10 we restricted the solution to number pairs where the power balance is achieved to within 5 or 10 kW from an input power of 0.3 to 0.7 MW. The solution spaces for several equations that are based upon slightly different models of the physics in the region are shown in Fig. 10. On one model, the outside magnetic surface radiates all the input power so that even the Marfe is detached and, in the other model, there is some assumed impurity accumulation in the Marfe region. These solutions are picked out easily in LOCUS by using the CONSTRAINTS or SYMBOLS options to find points with $F < 0.005$ or $F < 0.01$.

The Marfe can be understood as solutions with large TH implying large differences in the electron temperature along a magnetic surface. We found that small differences in the electron temperature can occur at higher electron temperatures where parallel electron heat conduction dominates the energy balance and at electron temperatures around 30 eV (Fig. 12) where the detached plasma has performed. The detached plasma is stable due to the positive slope on the curves of $P_{RAD}/n_e n_{imp}$ versus T_e curves for oxygen impurities (Ref. 8).

Again, the main utility of the LOCUS data base program for solving this equation was the power of its graphical and statistical packages for solving, understanding, and displaying the component behavior. Plots of the components of the power balance and variations to the physics assumptions were readily implemented and displayed. Different physics quantities could be generated easily with the expression tables in LOCUS. Moreover, the form of the solutions is readily understood and regions of many possible near-solutions are naturally exposed by the LOCUS treatment. Curve fitting, integration, and differentiation of the resultant parameters were easily accomplished with LOCUS.

Summary

This note has explored a different usage of the LOCUS data base program where the input is number pairs and the aim was to simulate images or solve equations rather than to analyze experimental data. We find that LOCUS (due to its flexibility, ease of use, graphics package, and statistical options) is a useful place to obtain a variety of results quickly. The availability of multiple expressions in LOCUS allowed the generation of many physical parameters starting from ordered and random input numbers.

Acknowledgment

This work was supported by the U.S. Department of Energy Contract No. DE-AC02-76-CHO-3073.

References

[1]J.A. Murphy, Princeton Plasma Physics Laboratory Report PPPL-TM-364-R (1986).

[2]J.A. Murphy and R. Wieland, Rev. Sci. Instrum. **59**, 1780 (1988).

[3]M. Abramowitz and I. Stegun, "Handbook of Mathematical Functions," (Dover Publications, Inc., New York City, 1965), p. 991-995.

[4]S. Medley, Rev. Sci. Instrum. **56**, 1873 (1985).

[5]J.D. Strachan et al., Proc. European Conf. on Plasma Physics and Controlled Fusion, Budapest, Hungary (1985), p.155.

[6]J.D. Strachan et al., Bull. Am. Phys. Soc. **32**, 1742 (1987).

[7]J.F. Drake, University of Maryland Plasmas Preprint UMPLFP No. 87-020 (1986).

[8]B. Lipschultz et al., Nucl. Fusion **24**, 977 (1984).

Figures

FIG. 1. The sequenced number pairs PH1 and TH plotted against each other. Each point is a separate record (entry) in the PICT1 LOCUS data base.

FIG. 2. The random number RA plotted against the sequenced number PH1.

FIG. 3. The random number RA plotted against the sequenced number TH.

FIG. 4. The plasma TV images: (a) view of the vacuum vessel, (b) a small plasma initially having contact on the moveable limiter and later in the same exposure having contact with the inner wall limiter, (c) image simulation of a plasma having uniform edge emissivity, and (d) a detached plasma.

FIG. 5. Image simulation of a detached plasma using PICT2 with the sequenced number pairs as input.

FIG. 6. Image simulation of a detached plasma using PICT1 with the sequenced number pairs and the random number as inputs to distribute the plasma emissivity on the plasma surface.

FIG. 7. Image simulation of a cylinder using PICT1 with the sequenced number pairs and the random numbers as inputs.

FIG. 8. Image simulation as done in Fig. 6 but with the data points (plasma emissivity) distributed uniformly inside the plasma volume.

FIG. 9. Value of the Power balance equation F1 (in units of MW) at constant PH1 (or $T1$ or time) and as a function of TH (or $T2$). Solution of the equation is obtained at $F1 = 0$.

FIG. 10. The space of the sequenced number pairs (PH1,TH) which are solutions to the power balance equation. The solutions are identified by the constraints or symbols indicating that the equation is close to zero (and, therefore, is a solution). Several versions of the power balance are indicated by F, F1, and F2. Each version makes a different assumption about the physics occurring in the radiating layer.

FIG. 11. The same solutions represented in Fig. 10 but with the axes representing physical quantities. $T1$ is the electron temperature in the non-Marfe region. $T2$ is the electron temperature in the Marfe region (shown under the physical assumptions of two of the equations). $T1 > T2$ is an indication of the MARFE. $T1 \simeq T2$ at ~ 0.18 sec is an indication of the uniformly radiating edge or detached plasma.

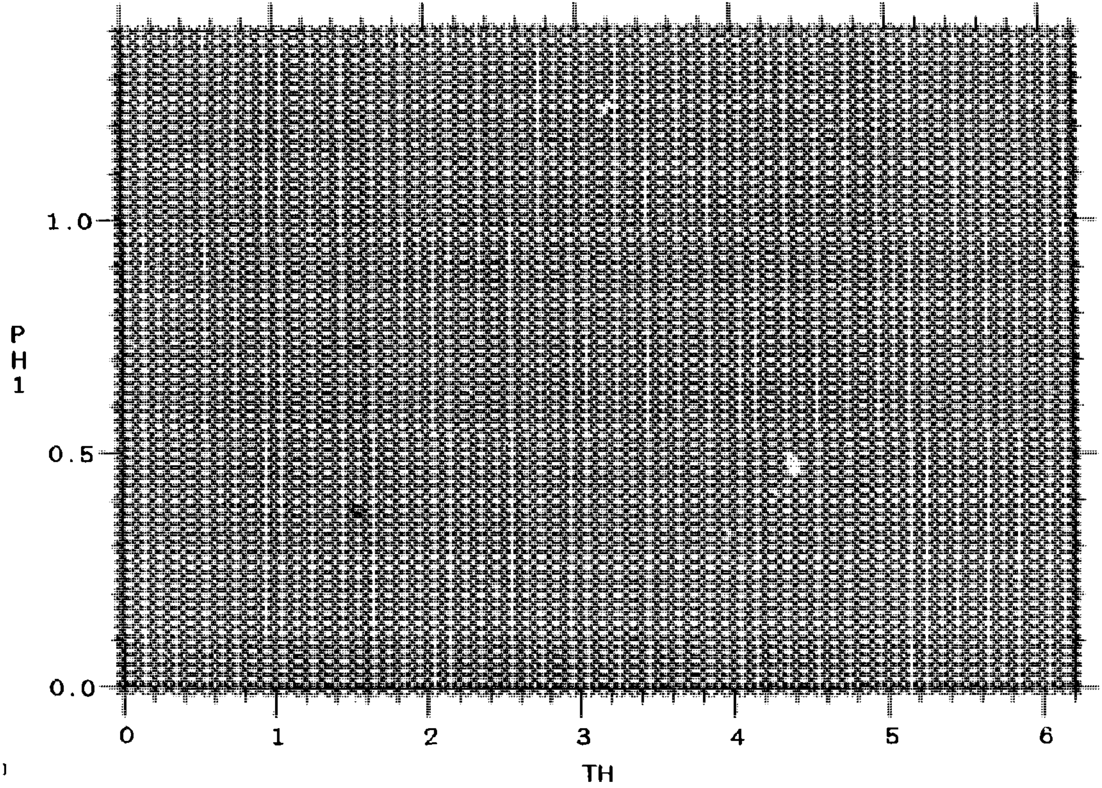

FIG. 1

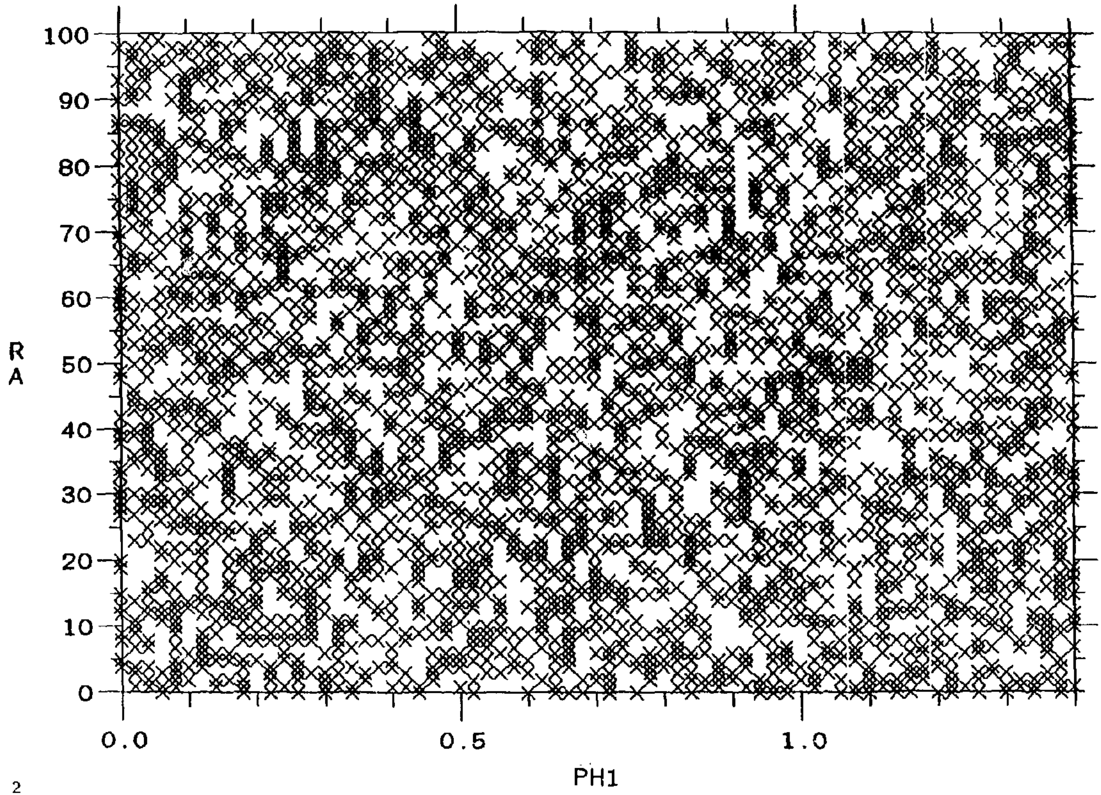

FIG. 2

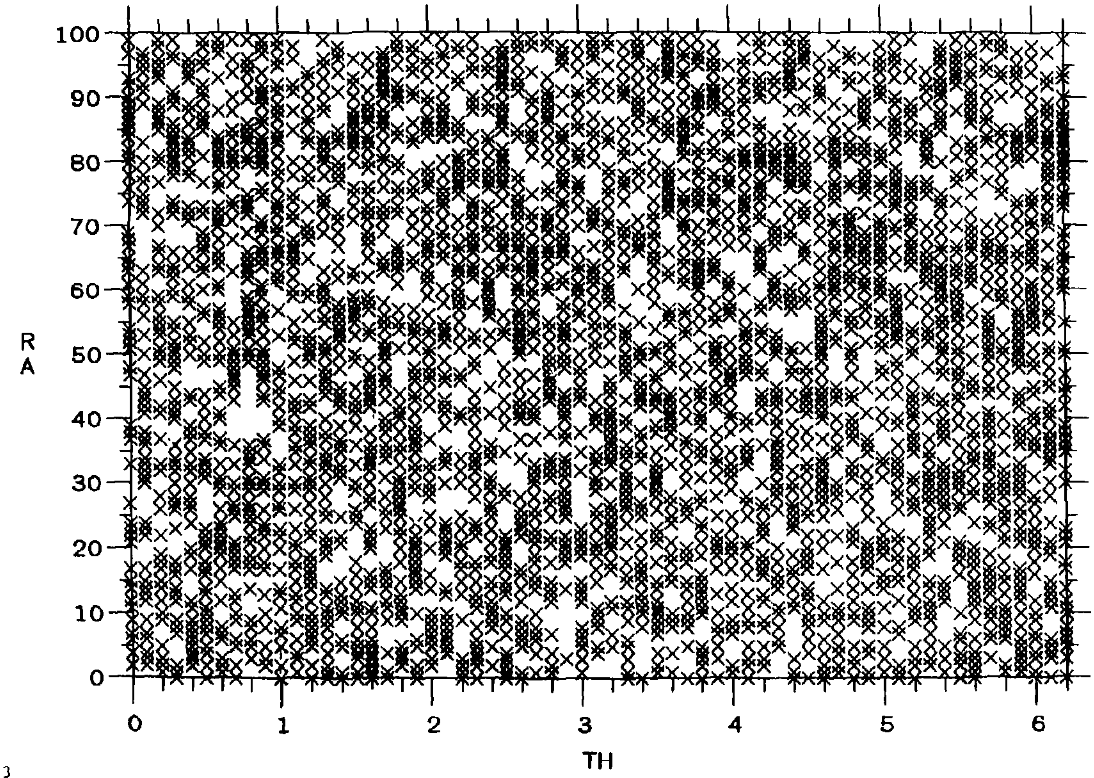

FIG. 3

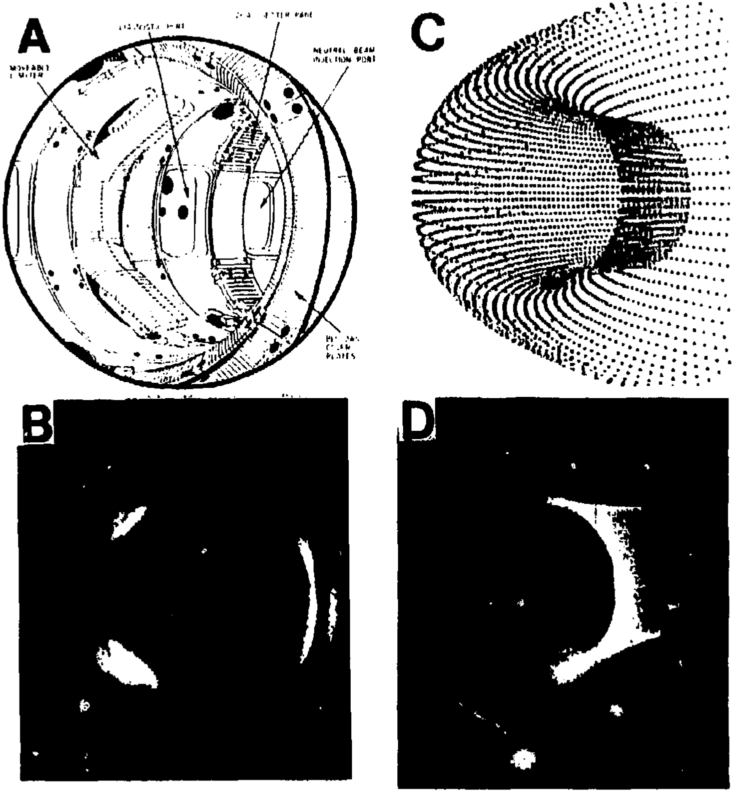

FIG. 4

15

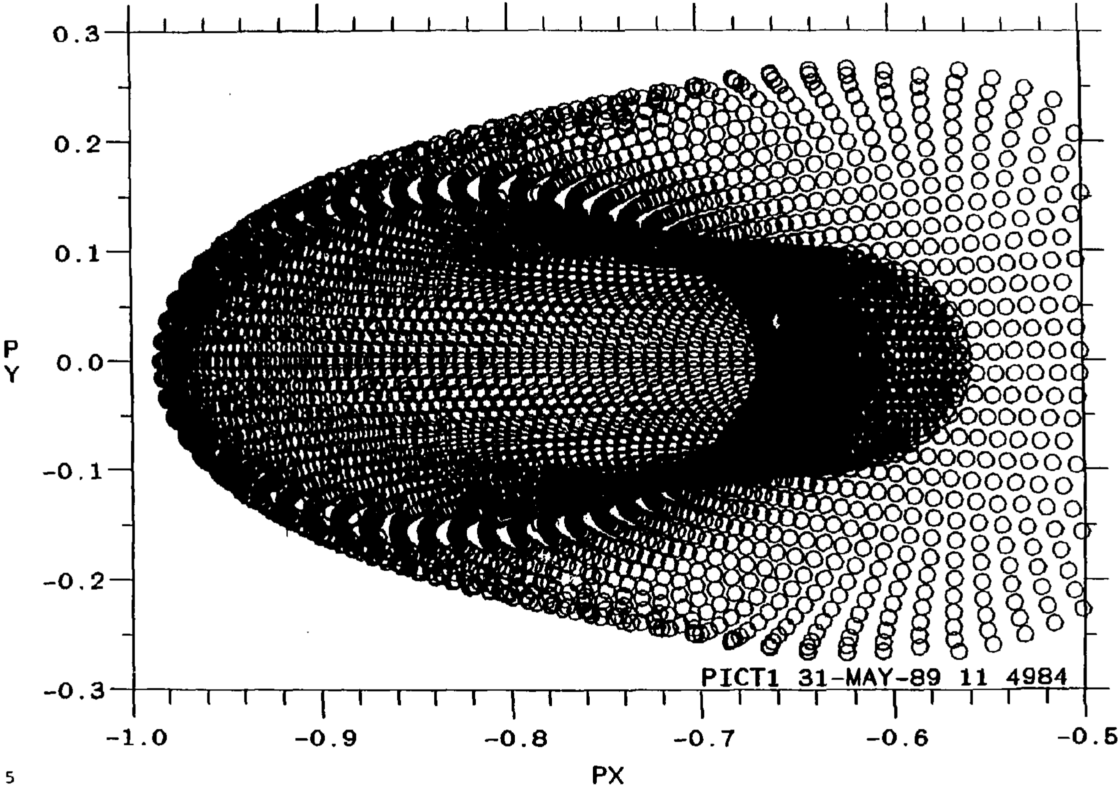

FIG. 5

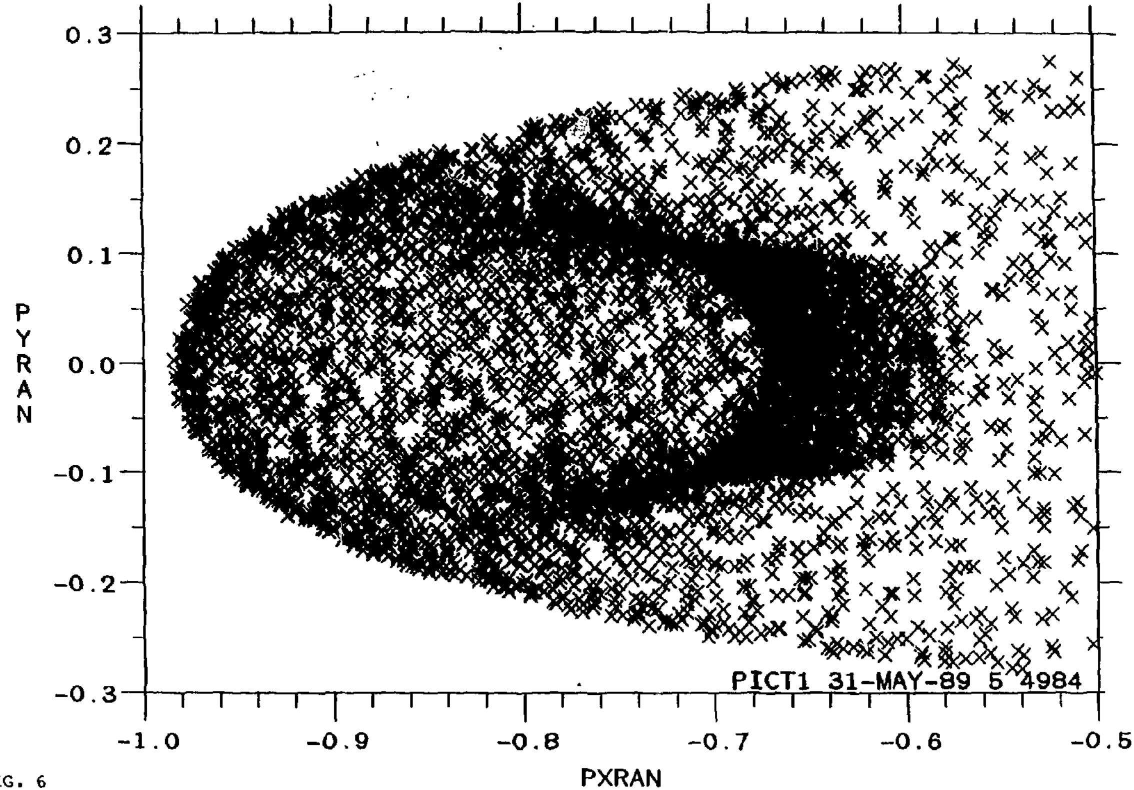
0.3
0.2
0.1
0.0
-0.1
-0.2
-0.3
PYRAN
-1.0
-0.9
-0.8
-0.7
-0.6
-0.5
PXRAN
PICT1 31-MAY-89 5 4984

FIG. 6

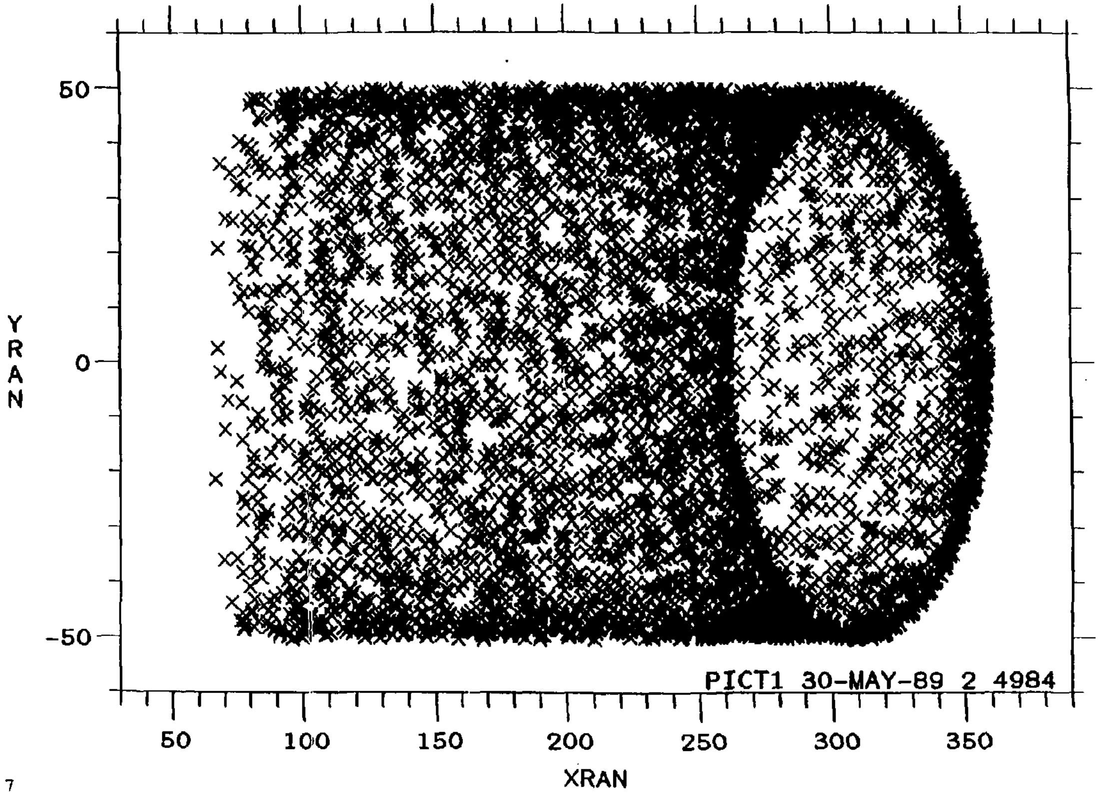
50
0
-50
YRAN
PICT1 30-MAY-89 2 4984
50
100
150
200
250
300
350
XRAN

FIG. 7

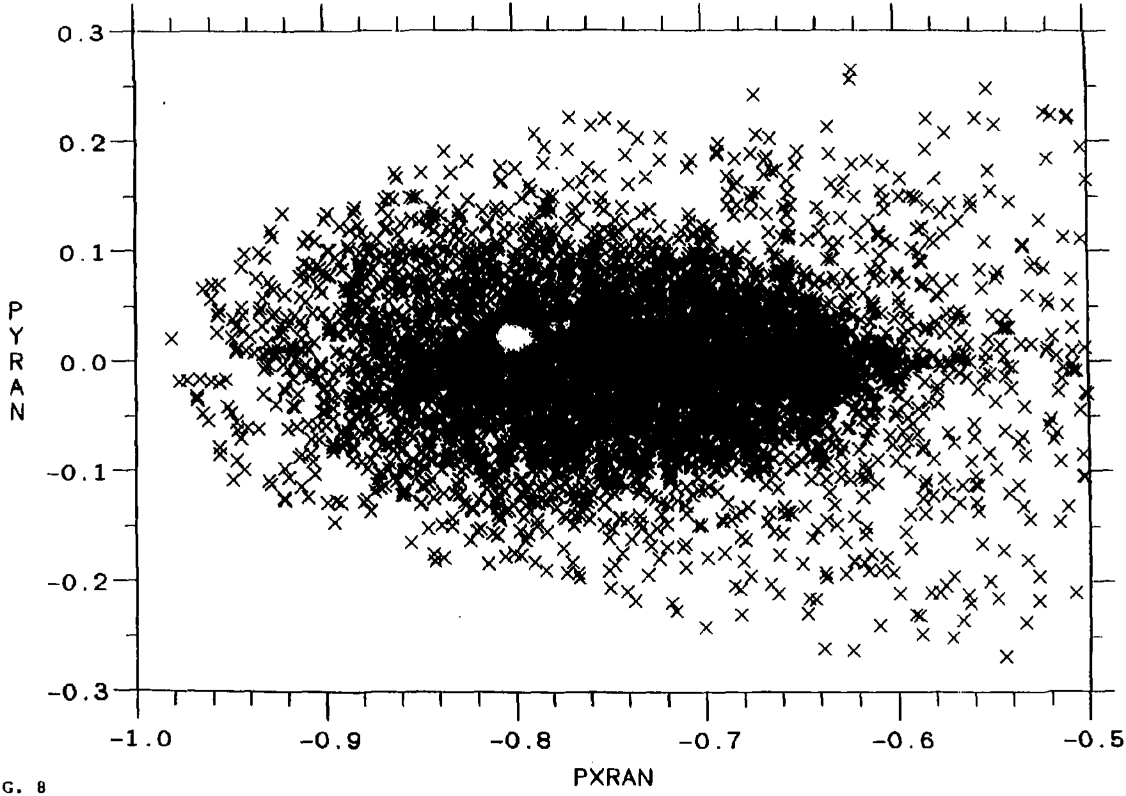

FIG. 8

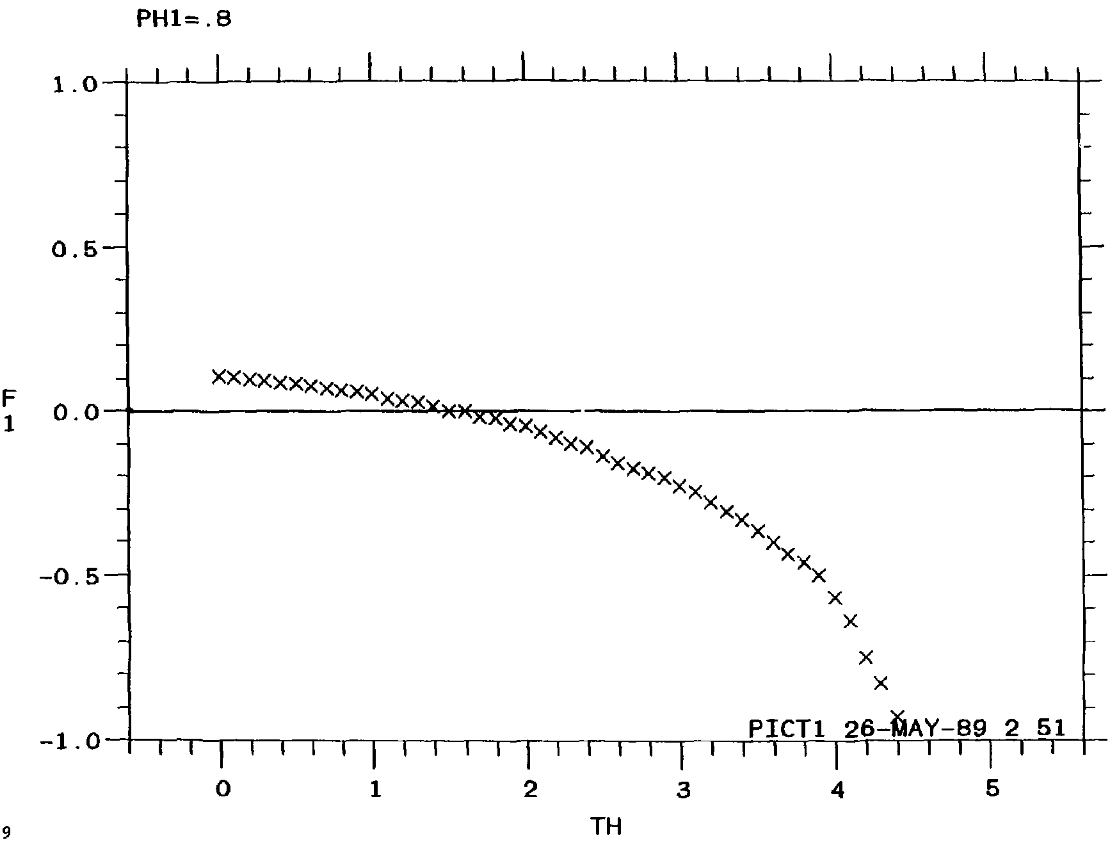

FIG. 9

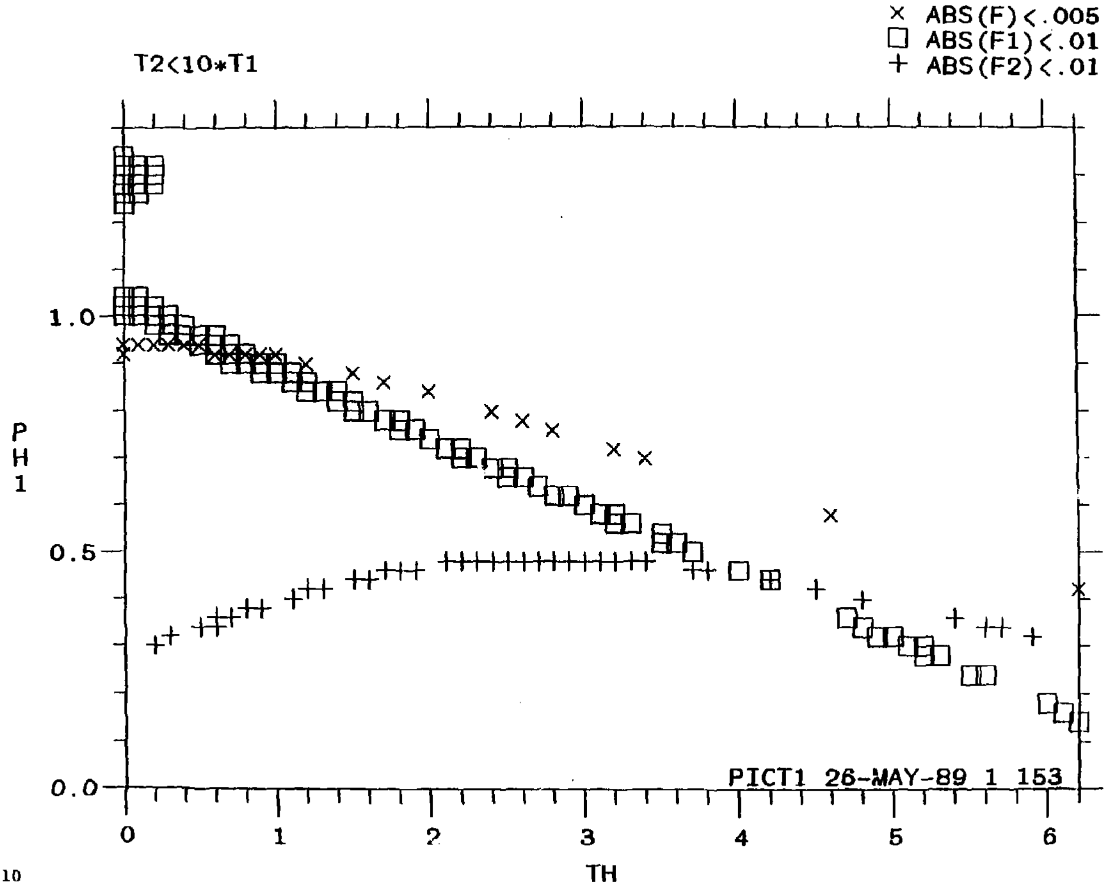
× ABS(F)<.005
□ ABS(F1)<.01
+ ABS(F2)<.01
T2<10*T1
PHI
1.0
0.5
0.0
0
1
2
3
4
5
6
TH
PICT1 26-MAY-89 1 153

FIG. 10

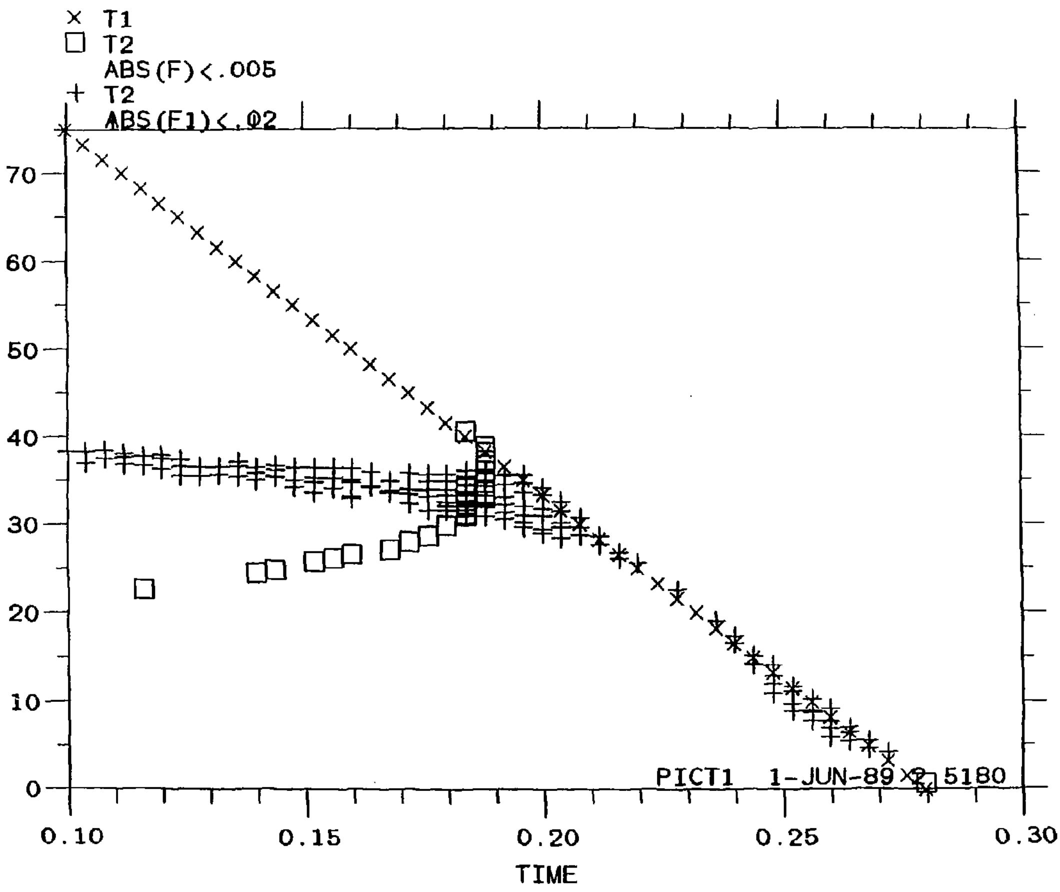
× T1
□ T2
ABS(F)<.005
+ T2
ABS(F1)<.02
0
10
20
30
40
50
60
70
0.10
0.15
0.20
0.25
0.30
TIME
PICT1 1-JUN-89 5180

FIG. 11

EXTERNAL DISTRIBUTION IN ADDITION TO UC-420

Dr. Frank J. Paoloni, Univ of Wollongong, AUSTRALIA
Prof. M.H. Brennan, Univ Sydney, AUSTRALIA
Plasma Research Lab., Australian Nat. Univ., AUSTRALIA
Prof. I.R. Jones, Flinders Univ., AUSTRALIA
Prof. F. Cap, Inst Theo Phys, AUSTRIA
Prof. M. Heindler, Instut für Theoretische Physik, AUSTRIA
M. Goossens, Astronomisch Instituut, BELGIUM
Ecole Royale Militaire, Lab de Phys Plasmas, BELGIUM
Commission-European, Dg-XII Fusion Prog, BELGIUM
Prof. R. Boucique, Rijksuniversiteit Gent, BELGIUM
Dr. P.H. Sakanaka, Instituto Fisica, BRAZIL
Instituto De Pesquisas Espaciasi-INPE, BRAZIL
Documents Office, Atomic Energy of Canada Limited, CANADA
Dr. M.P. Bachynski, MPB Technologies, Inc., CANADA
Dr. H.M. Skarsgard, University of Saskatchewan, CANADA
Dr. H. Barnard, University of British Columbia, CANADA
Prof. J. Teichmann, Univ. of Montreal, CANADA
Prof. S.R. Sreenivasan, University of Calgary, CANADA
Prof. Tudor W. Johnston, INRS-Energie, CANADA
Dr. Bolton, Centre canadien de fusion magnetique, CANADA
Dr. C.R. James, Univ. of Alberta, CANADA
Dr. Peter Lukac, Komenskeho Univ, CZECHOSLOVAKIA
The Librarian, Culham Laboratory, ENGLAND
The Librarian, Rutherford Appleton Laboratory, ENGLAND
Mrs. S.A. Hutchinson, JET Library, ENGLAND
C. Mouttet, Lab. de Physique des Milieux Ionises, FRANCE
J. Radet, CEN/CADARACHE - Bat 506, FRANCE
Ms. C. Rinni, Librarian, Univ. of Ioannina, GREECE
Dr. Tom Mual, Academy Bibliographic Ser., HONG KONG
Preprint Library, Hungarian Academy of Sciences, HUNGARY
Dr. B. Das Gupta, Saha Inst of Nucl. Phys., INDIA
Dr. P. Kaw, Institute for Plasma Research, INDIA
Dr. Philip Rosenau, Israel Inst. of Tech, ISRAEL
Librarian, Int'l Ctr Theo Phys, ITALY
Prof. G. Rostagni, Istituto Gas Ionizzati Del CNR, ITALY
Miss Clelia De Palo, Assoc EURATOM-ENEA, ITALY
Dr. G. Grosso, Istituto di Fisica del Plasma, ITALY
Dr. H. Yamato, Toshiba Res & Dev, JAPAN
Prof. I. Kawakami, Atomic Energy Res. Institute, JAPAN
Prof. Kyoji Nishikawa, Univ of Hiroshima, JAPAN
Director, Dept. Large Tokamak Res. JAERI, JAPAN
Prof. Satoshi Itoh, Kyushu University, JAPAN
Research Info Center, Nagoya University, JAPAN
Prof. S. Tanaka, Kyoto University, JAPAN
Library, Kyoto University, JAPAN
Prof. Nobuyuki Inoue, University of Tokyo, JAPAN
S. Mori, JAERI, JAPAN
H. Jeong, Librarian, Korea Advanced Energy Res Inst, KOREA
Prof. D.I. Choi, The Korea Adv. Inst of Sci & Tech, KOREA
Prof. B.S. Liley, University of Waikato, NEW ZEALAND
Institute of Plasma Physics, PEOPLE'S REPUBLIC OF CHINA
Librarian, Institute of Phys., PEOPLE'S REPUBLIC OF CHINA
Library, Tsing Hua University, PEOPLE'S REPUBLIC OF CHINA
Z. Li, Southwest Inst. Physics, PEOPLE'S REPUBLIC OF CHINA
Prof. J.A.C. Cabral, Inst Superior Tecnico, PORTUGAL
Dr. Octavian Petrus, AL I CUZA University, ROMANIA
Dr. Jam de Villiers, Fusion Studies, AEC, SO AFRICA
Prof. M.A. Hellberg, University of Natal, SO AFRICA
C.I.E.M.A.T., Fusion Div. Library, SPAIN
Dr. Lennart Stenflo, University of UMEA, SWEDEN
Library, Royal Institute of Tech, SWEDEN
Prof. Hans Wilhelmson, Chalmers Univ of Tech, SWEDEN
Centre Phys des Plasmas, Ecole Polytech Fed, SWITZERLAND
Bibliotheek, Fom-Inst Voor Plasma-Fysica, THE NETHERLANDS
Metin Durgut, Middle East Technical University, TURKEY
Dr. D.D. Ryutov, Siberian Acad Sci, USSR
Dr. G.A. Eliseev, Kurchatov Institute, USSR
Dr. V.A. Glukhikh, Inst Electrophysical Apparatus, USSR
Prof. O.S. Padichenko, Inst. of Phys. & Tech. USSR
Dr. L.M. Kovrizhnykh, Institute of Gen. Physics, USSR
Nuclear Res. Establishment, Julich Ltd., W. GERMANY
Bibliothek, Inst. Fur Plasmaforschung, W. GERMANY
Dr. K. Schindler, Ruhr-Universitat Bochum, W. GERMANY
ASDEX Reading Rm, c/o Wagner, IPP/Max-Planck, W. GERMANY
Librarian, Max-Planck Institut, W. GERMANY
Prof. R.K. Janev, Inst of Phys, YUGOSLAVIA